Astron. Astrophys. 362, 325–332 (2000)

ASTRONOMY AND ASTROPHYSICS

On the oxygen abundance determination in H II regions

The problem of the line intensities – oxygen abundance calibration

L.S. Pilyugin

Main Astronomical Observatory of National Academy of Sciences of Ukraine, Goloseevo, 03680 Kiev-127, Ukraine (pilyugin@mao.kiev.ua)

Received 18 February 2000 / Accepted 21 March 2000

Abstract. The problem of the line intensities – oxygen abundance calibration has been considered. We confirm the idea of McGaugh (1991) that the strong oxygen lines ($[OII]\lambda\lambda 3727,3729$ and $[OIII]\lambda\lambda 4959,5007$) contain the necessary information for determination of accurate abundances in low-metallicity (and may be also in high-metallicity) H II regions. It has been found that the excitation parameters p_3 or p_2 (which are defined here as contributions of the radiation in $[OIII]\lambda\lambda 4959,5007$ lines and in $[OII]\lambda\lambda 3727,3729$ lines to the "total" oxygen radiation respectively) allow to take into account the variations in R_{23} values among H II regions with a given oxygen abundance. Based on this fact a new way of the oxygen abundance determination in H II regions (p – method) has been constructed and corresponding relations between $[OII]\lambda\lambda 3727,3729$, $[OIII]\lambda\lambda 4959,5007$ line intensities and the oxygen abundance have been derived empirically using the available oxygen abundances determined via measurement of temperature-sensitive line ratios (T_e – method).

In parallel a new R_{23} calibration has been derived on the base of recent data and compared to previous calibrations. For oxygen-rich H II regions the present R_{23} calibration is close to that of Edmunds & Pagel (1984): their calibration has the same slope but is shifted towards higher oxygen abundances by around 0.07 dex as compared to the present calibration.

Key words: ISM: H II regions – galaxies: abundances – galaxies: ISM – galaxies: irregular – galaxies: spiral

1. Introduction

The oxygen abundance is one of the fundamental characteristics of a galaxy. The radial distribution of the oxygen abundance in a galaxy (together with radial distributions of gas and star surface mass densities) provides a strong constraint on models of (chemical) evolution. In the general case the intensities of oxygen emission lines in spectra of H II regions depend not only on the oxygen abundance but also on physical conditions. The oxygen abundance can be derived from accurate measurement of temperature-sensitive line ratios, such as $[OIII]\lambda\lambda 4959,5007/\lambda 4363$. This method will be referred to as the T_e – method.

Unfortunately, in oxygen–rich H II regions the temperature-sensitive lines like $[OIII]\lambda 4363$ are too weak to be detected. For such H II regions empirical abundance indicators based on more readily observable lines were suggested (Pagel et al. 1979, Alloin et al. 1979). The empirical oxygen abundance indicator $R_{23} = (I_{[OII]\lambda 3727,\lambda 3729} + I_{[OIII]\lambda 4959,\lambda 5007})/I_{H\beta}$ suggested by Pagel et al. (1979) has found widespread acceptance and use for the oxygen abundance determination in H II regions where the temperature-sensitive lines are undetectable. This method will be referred to as the R_{23} – method. Several workers have suggested calibrations of R_{23} in terms of oxygen abundance (Edmunds & Pagel 1984, McCall et al. 1985, Dopita & Evans 1986, Zaritsky et al. 1994, among others). Zaritsky et al's calibration is an average of the three former calibrations.

The oxygen abundances of H II regions in many irregular galaxies are derived with the T_e – method. Those in H II regions of the Milky Way have also been determined with the T_e – method (Shaver et al. 1983). This data is a base for many investigations of chemical evolution of our Galaxy. Oxygen abundances in H II regions of many spiral galaxies have been derived with the R_{23} – method. As indicated by Skillman et al. (1996), the precise choice of the O/H – R_{23} calibration is not critical in differential comparisons of the abundance properties of different objects if the oxygen abundances in all the objects are derived with the same O/H – R_{23} calibration. However, the comparison of the abundance properties of galaxies where the oxygen abundances were determined with the T_e – method (irregular galaxies, Milky Way and a few other spiral galaxies) and galaxies where the oxygen abundances were determined with the R_{23} – method (spiral galaxies) is justified only if the two methods agree. The existing O/H – R_{23} calibrations (Edmunds & Pagel 1984, McCall et al. 1985, Dopita & Evans 1986, McGaugh 1991) are based on then-available oxygen abundance determinations through the T_e – method and H II region models, whereas more oxygen abundance determinations through the T_e – method are available now. Then the existing O/H – R_{23} calibrations should be verified in the light of more recent data and a new calibration derived if necessary.

The search for a line intensities – O/H calibration which results in the same oxygen abundances as the T_e – method is the goal of this study. The line intensities – O/H calibration has

been derived in Sect. 2. A discussion will be presented in Sect. 3. Sect. 4 is a brief summary.

2. Line intensities – O/H calibration

In order to check whether the T_e – method and the R_{23} – method result in the same oxygen abundances the X_{23}(= log R_{23}) versus 12 + logO/H diagram for the Milky Way Galaxy H II regions from Shaver et al. (1983) and H II regions in spiral and irregular galaxies together with O/H – R_{23} calibrations after Edmunds & Pagel 1984, McCall et al. 1985, Dopita & Evans 1986, and Zaritsky et al. 1994 has been constructed, Fig. 1. The data for H II regions in irregular galaxies were taken from (Izotov & Thuan 1998, 1999: Izotov et al. 1994, 1997; Kobulnicky & Skillman 1996, 1997, 1998: Kobulnicky et al. 1997; Skillman et al. 1994; Thuan et al. 1995; Vilchez & Iglesias-Paramo 1998). The data for H II regions in spiral galaxies were taken from (Esteban et al. 1998; Esteban et al. 1999a,b; Garnett et al. 1999; Gonzalez-Delgado et al. 1995; Kwitter & Aller 1981; Pagel et al. 1980; Peimbert et al. 1993; Shaver et al. 1983; Shields & Searle 1978; van Zee et al. 1998; Vilchez & Esteban 1996; Vilchez et al. 1988; Webster & Smith 1983). These lists (involving 151 data points) do not pretend to be exhaustive ones. In the case of low-metallicity H II regions there is a large set of data with recent high-quality determinations of oxygen abundance with the T_e – method, therefore earlier ones were not included in our list. In the case of high-metallicity H II regions there are a few recent high-quality determinations of the oxygen abundance with the T_e – method, therefore we have to include in our list all available oxygen abundance determinations although some data were obtained around 20 years ago. In a few cases there are two independent determinations of the oxygen abundance in the same object or independent determinations in different parts of the H II region. Since the goal of the present study is a search for the line intensities – oxygen abundance relation but not an investigation of the chemical properties of individual galaxies, the independent determinations of oxygen abundance in the same object were included in the list as individual data points. Our data confirm the conclusion of Kennicutt et al. (2000) that the Edmunds and Pagel calibration (Edmunds & Pagel 1984) provides a more robust diagnostic of oxygen abundance, but an inspection of the Fig. 1 shows that it still results in an oxygen abundance that is higher than the mean at any given logR_{23}. Thus, none of the existing R_{23} – O/H calibration can reproduce the available data well enough and a new one should be constructed.

The simplest way to construct the line intensities – O/H relation is a traditional approach: to find a best fit R_{23} – O/H relation using available H II regions in which oxygen abundances were determined with the T_e – method. A one-to-one correpondence between the oxygen abundance and the R_{23} value is implied in this approach, i.e. the variations in R_{23} values among H II regions with a given oxygen abundance are not taken into consideration. However, McGaugh (1991) pointed out that the geometrical factor is important in low-metallicity H II regions and R_{23} must be supplemented with additional information. This can be verified in the following simple way. Let us consider the X_2 versus p_2 and X_3 versus p_3 diagrams, Figs. 2, 3. (The following notations will be accepted here: $R_2 = I_{[OII]\lambda3727+\lambda3729}/I_{H\beta}$, X_2 = logR_2, $R_3 = I_{[OIII]\lambda4959+\lambda5007}/I_{H\beta}$, X_3 = logR_3, R_{23} =R_2 + R_3, X_{23} = logR_{23}, p_2 = X_2 - X_{23}, and p_3 = X_3 - X_{23}.) If the value of R_{23} is constant for H II regions with similar oxygen abundances, then the H II regions with similar oxygen abundances should lie along a straight line with a slope equal to 1 in the X_2 versus p_2 and X_3 versus p_3 diagrams. The positions of H II regions with oxygen abundances logO/H+12 in the range from 7.1 to 7.3 are shown by circles, in the range interval from 7.4 to 7.6 are shown by triangles, and in the range interval from 8.0 to 8.1 are shown by plusses, Figs. 2, 3. The linear best fits to corresponding data are presented by solid lines. Dashed lines are lines with a slope equal to 1. Inspection of Figs. 2, 3 shows that the H II regions with similar oxygen abundances lie indeed along a straight line, but a slope of this straight line is not equal to 1.

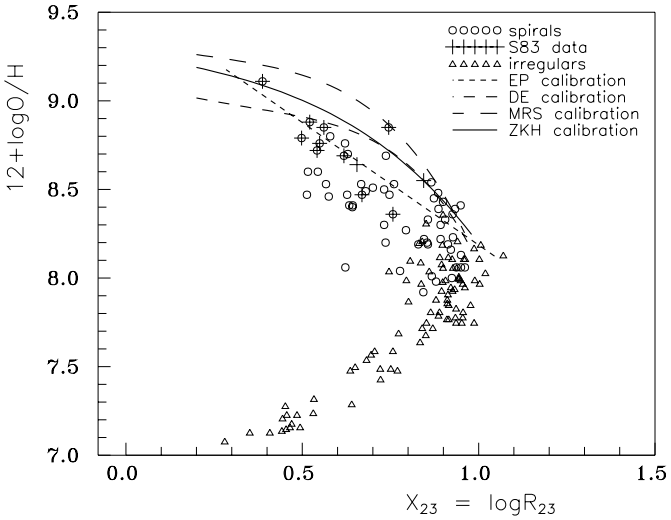

Fig. 1. The OH – logR_{23} diagram. The positions of H II regions in spiral galaxies (circles) (the H II regions in our Galaxy from Shaver et al. 1983 (S83) are indicated by plusses) and in irregular galaxies (triangles) are shown together with OH – R_{23} calibrations of different authors: Edmunds & Pagel 1984 (EP), McCall et al. 1985 (MRS), Dopita & Evans 1986 (DE), and Zaritsky et al. 1994 (ZKH).

The fact that the slope of the best fit differs from 1 has far-reaching implications: it means that value of $logR_{23}$ varies systematically with p_3 and a quantity other than $logR_{23}$ should be used in oxygen abundance determination. In order to verify the reality of this fact and to clearly recognize the consequences, the subset of selected H II regions with best determined oxygen abundances through the T_e – method has been considered. This subset includes the low-metallicity (12+logO/H $<$ 7.95) H II regions from Izotov & Thuan (1998, 1999) and Izotov et al. (1994, 1997). Since the H II regions with similar oxygen abundances lie along a straight line with a slope other than unity the extrapolated intersect X_3 is not equal to R_{23}. The notation X_3^* will denote the value of X_3 extrapolated to p_3 = 0. Similarly, the notation X_2^* will be adopted for the value of X_2 extrapolated

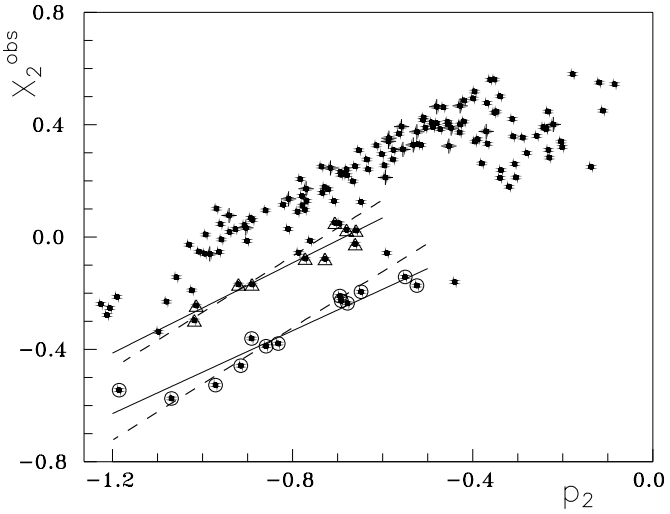

Fig. 2. The p_2 versus X_2 diagram for H II regions in spiral and irregular galaxies (points). The positions of H II regions with 7.1 ≤ 12+log(O/H)$_{Te}$ ≤ 7.3 are shown by circles, H II regions with 7.4 ≤ 12+log(O/H)$_{Te}$ ≤ 7.6 are shown by triangles, H II regions with 8.0 ≤ 12+log(O/H)$_{Te}$ ≤ 8.1 are shown by plusses. Solid lines are best fits to positions of H II regions with 7.1 ≤ 12+log(O/H)$_{Te}$ ≤ 7.3 and H II regions with 7.4 ≤ 12+log(O/H)$_{Te}$ ≤ 7.6. Dashed lines are lines with slope equal to 1.

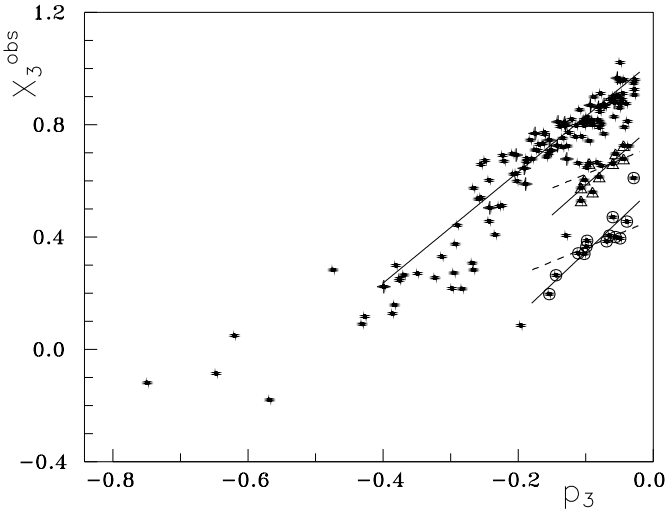

Fig. 3. The p_3 versus X_3 diagram for H II regions in spiral and irregular galaxies (points). The positions of H II regions with 7.1 ≤ 12+log(O/H)$_{Te}$ ≤ 7.3 are shown by circles, H II regions with 7.4 ≤ 12+log(O/H)$_{Te}$ ≤ 7.6 are shown by triangles, H II regions with 8.0 ≤ 12+log(O/H)$_{Te}$ ≤ 8.1 are shown by plusses. Solid lines are best fits to positions of H II regions with 7.1 ≤ 12+log(O/H)$_{Te}$ ≤ 7.3, H II regions with 7.4 ≤ 12+log(O/H)$_{Te}$ ≤ 7.6, and H II regions with 8.0 ≤ 12+log(O/H)$_{Te}$ ≤ 8.1. Dashed lines are lines with slope equal to 1.

to p_2 = 0. The data for the selected subset of H II regions result in the following relation between $\Delta X_3 = X_3^{obs} - X_3^*$ and Δp_3

$$\Delta X_3 = 2.20\ \Delta p_3 = 2.20\ p_3, \quad (1)$$

where $\Delta p_3 = p_3$ by virtue of $p_3^* = 0$ was adopted. The corresponding relation between $\Delta X_2 = X_2^{obs} - X_2^*$ and $\Delta p_2 = p_2$ is given by equation

$$\Delta X_2 = 0.76\ \Delta p_2 = 0.76\ p_2. \quad (2)$$

Using these equations the values of X_3^* and X_2^* have been computed for all the H II regions from the selected subset.

The oxygen abundances (O/H)$_{Te}$ versus observed X_{23} and versus computed X_2^* and X_3^* values for the selected subset of H II regions are shown in Fig. 4. The O/H versus X_2^* diagram is presented by triangles, the O/H versus X_3^* diagram is presented by points, and the O/H versus X_{23} diagram is presented by plusses. The solid line is the best fit to the O/H versus X_3^* relation, the dashed line is the best fit to the O/H versus X_{23} relation. The X_{23} values are positioned between corresponding X_2^* and X_3^* values. Since p_3 values are more close to zero than p_2 values the extrapolated intersect X_3 seem to be more reliable than X_2. Inspection of Fig. 4 shows that linear approximations are acceptable for the relations between O/H and X_{23} and between O/H and X_3^*. Thus, the values of X_{23} and X_3^* have been calibrated in terms of oxygen abundance using the linear approximation. The best fits to the data result in the following relations (Fig. 4)

$$12 + log(O/H)_{R_{23}} = 6.53 + 1.40\ X_{23}, \quad (3)$$

$$12 + log(O/H)_{P_3} = 6.35 + 1.45\ X_3^*. \quad (4)$$

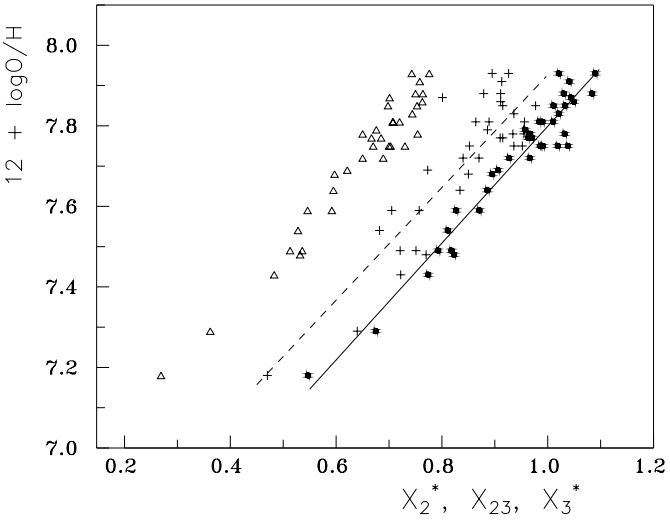

Fig. 4. The oxygen abundances (O/H)$_{Te}$ versus observed X_{23} and computed X_2^* and X_3^* values for selected subset of galaxies with best defined oxygen abundances. The O/H versus X_2^* diagram is presented by triangles, the O/H versus X_3^* diagram is presented by points, and the O/H versus X_{23} diagram is presented by plusses The solid line is the best fit to the O/H versus X_3^* relation, the dashed line is the best fit to the O/H versus X_{23} relation.

Using these equations two values of the oxygen abundance $(O/H)_{R_{23}}$ and $(O/H)_{P_3}$ have been obtained for every H II region in the selected subset. The determination of the oxygen abundance through p_3 (or p_2) will be referred to as the p – method.

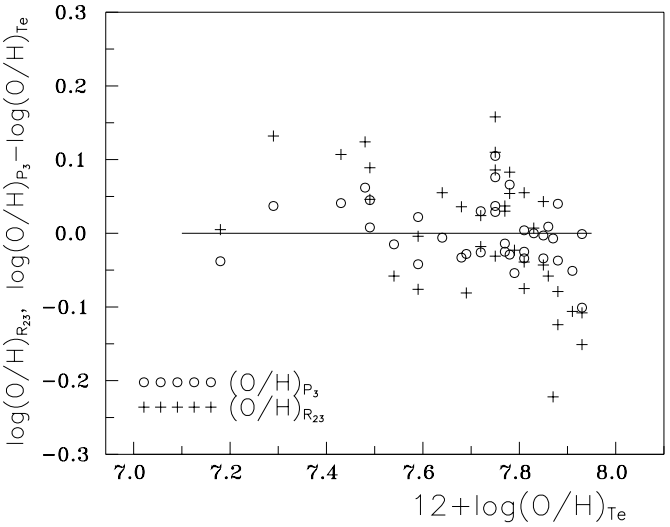

Fig. 5. The differences between oxygen abundances derived with the suggested p – method and derived with the T_e – method (circles) and differences between oxygen abundances derived with the R_{23} – method and derived with the T_e – method (crosses) for selected subset of H II regions in irregular galaxies with best determined oxygen abundances (O/H)$_{Te}$.

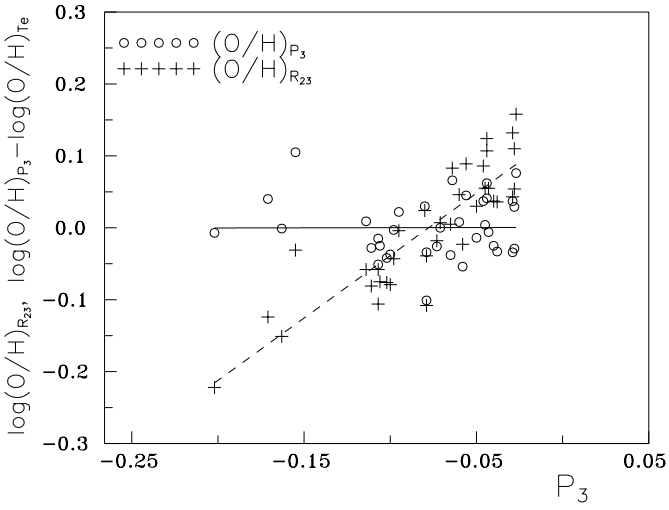

Fig. 6. The differences between oxygen abundances derived with the suggested p – method and derived with the T_e – method (circles) and differences between oxygen abundances derived with the R_{23} – method and derived with the T_e – method (plusses) as a function of parameter p_3 for selected subset of H II regions in irregular galaxies with best determined oxygen abundances through the Te – method. The solid line is the best fit $\Delta log(O/H)_{P_3} - p_3$ relation, the dashed line is the best fit $\Delta log(O/H)_{R_{23}} - p_3$ relation.

The differences $\Delta log(O/H)_{R_{23}}$ between oxygen abundances $(O/H)_{R_{23}}$ derived with the R_{23} – method and oxygen abundances $(O/H)_{Te}$ derived with the T_e – method are shown in Fig. 5 by plusses as a function of $(O/H)_{Te}$. The differences $\Delta log(O/H)_{P_3}$ = $(O/H)_{P_3}$ - $(O/H)_{Te}$ are shown in Fig. 5 by circles. It can be seen in Fig. 5 that the mean value of $\Delta log(O/H)_{P_3}$ is appreciable lower ($\sim$ 0.042 dex) than the mean value of $\Delta log(O/H)_{R_{23}}$ ($\sim$ 0.086 dex).

The differences $\Delta log(O/H)_{P_3}$ and $\Delta log(O/H)_{R_{23}}$ as a function of p$_3$ are shown in Fig. 6. As seen in Fig. 6 the error in the value of the oxygen abundance derived with the R_{23} – method involves two parts: the first part is a random error comparable to the random error in the p – method, and the second part is a systematic error. The origin of this systematic error is as follows. In a general case the intensities of oxygen emission lines in spectra of H II regions depend not only on the oxygen abundance but also on the physical conditions (hardness of the ionizing radiation and geometrical factor). Then in the determination of the oxygen abundance from line intensities the physical conditions in the H II region should be taken into account. In the T_e – method this is done via T_e. In the p – method, physical conditions are allowed for via parameter p, i.e. the parameter p can be considered as some kind analogy of the electron temperature T_e in the oxygen abundance determination. In the R_{23} – method the physical conditions in H II region are ignored. Therefore, the oxygen abundances derived with the T_e – method and with the p – method involve only random errors (this is a strong argument that the physical conditions in H II region are well taken into account via parameter p), while the oxygen abundances derived with the R_{23} – method involve a systematic error caused by the failure to take into account the differences in physical conditions in different H II regions.

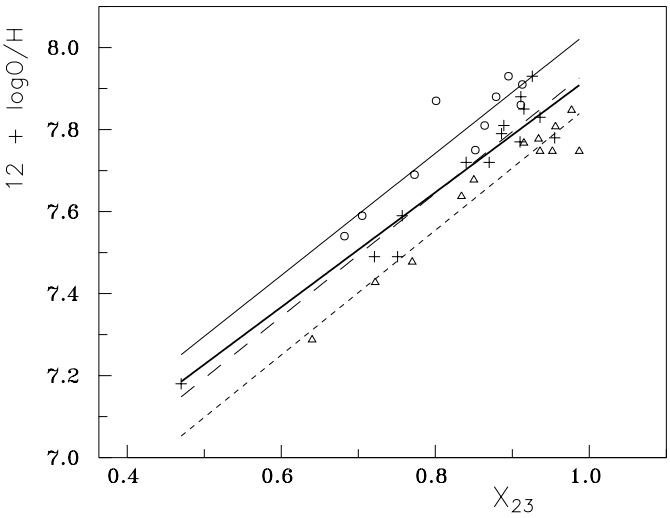

Fig. 7. The oxygen abundances (O/H)$_{Te}$ versus X$_{23}$ diagram for selected subset of galaxies with best defined oxygen abundances. The H II regions with $p_3 <$ –0.1 are shown by circles (and corresponding best fit is presented by the thin solid line), the H II regions with –0.05 $> p_3 >$ –0.1 are shown by plusses (and corresponding best fit is presented by the long-dashed line), the H II regions with $p_3 >$ –0.05 are shown by triangles (and corresponding best fit is presented by the short-dashed line). The thick solid line is the general best fit, i.e. best fit to all data (the same as in Fig. 4).

The fact that the value of $logR_{23}$ in H II regions with a given oxygen abundance varies systematically with p_3 can be directly established from detailed consideration of the X_{23} versus O/H diagram, Fig. 7. The H II regions with $p_3 <$ –0.1 are shown by circles (and corresponding best fit is presented by the thin

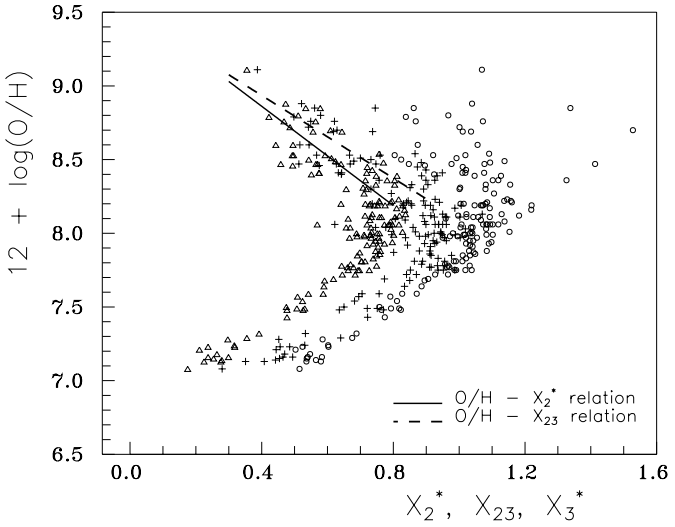

Fig. 8. The oxygen abundances (O/H)$_{Te}$ versus observed X$_{23}$ (plusses) and computed X$_2^*$ (triangles) and X$_3^*$ (circles) values for total set of H II regions in spiral and irregular galaxies. The solid line is the adopted O/H – X_2^* relation, the dashed line is the adopted O/H – X_{23} relation.

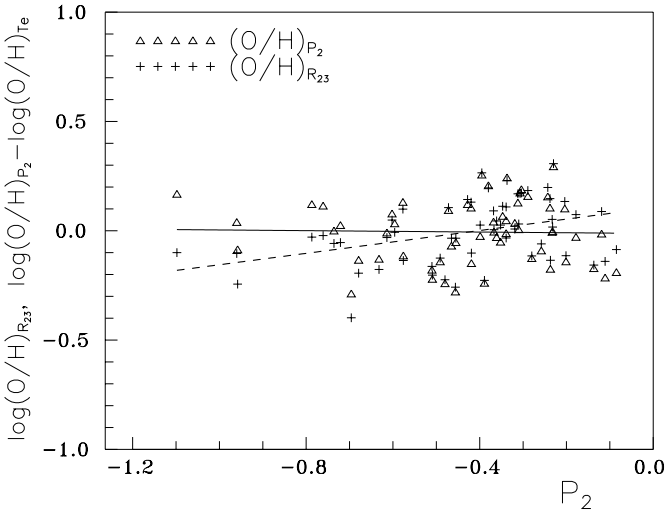

Fig. 9. The differences between oxygen abundances derived with the suggested p – method and derived with the T_e – method (triangles) and differences between oxygen abundances derived with the R_{23} – method and derived with the T_e – method (plusses) as a function of parameter p_2. The solid line is the best fit $\Delta log(O/H)_{P_2} - p_2$ relation, the dashed line is the best fit $\Delta log(O/H)_{R_{23}} - p_2$ relation.

solid line) in Fig. 7, the H II regions with –0.05 $> p_3 >$ –0.1 are shown by plusses (and corresponding best fit is presented by the long-dashed line), the H II regions with $p_3 >$ –0.05 are shown by triangles (and corresponding best fit is presented by the short-dashed line). The thick solid line in Fig. 7 is the general best fit, i.e. the best fit to all data (the same as in Fig. 4). Inspection of Fig. 7 shows that the H II regions with different values of p_3 lie along different straight lines shifted relative to each other depending on the value of p_3. According to the model grid of McGaugh (1991) this shifting is accounted for by the variations in the geometrical factors. The general best fit O/H – X$_{23}$ (Eq. (3)) is very close to the best fit to the data for H II regions with –0.05 $> p_3 >$ –0.1, Fig. 7. The H II regions with $p_3 >$ –0.05 are shifted to the right from the general best fit and as a consequence the $(O/H)_{R_{23}}$ values derived in these H II regions with Eq. (3) are higher than $(O/H)_{Te}$, Fig. 6. Conversely, the H II regions with $p_3 <$ –0.10 are shifted to the left from the general best fit in Fig. 7, and so the $(O/H)_{R_{23}}$ derived for them from Eq. (3) are lower than $(O/H)_{Te}$, Fig. 6.

Thus, the above discussion of the subset of selected H II regions with best determined oxygen abundances through the T_e – method suggests that *i)* the oxygen abundances derived with the R_{23} – method involve a systematic error caused by the failure to take into account the differences in physical conditions in different H II regions, *ii)* the physical conditions in H II region are well taken into account via the parameter p, and there is no systematic error in the oxygen abundances derived with the p – method. We confirm the idea of McGaugh (1991) that the strong oxygen lines ($[OII]\lambda\lambda 3727, 3729$ and $[OIII]\lambda\lambda 4959, 5007$) contain the necessary information for determination of accurate abundances in low-metallicity H II regions.

McGaugh (1991) has found that all the models converge toward the same upper branch line, R_{23} being relatively insensitive to geometrical factor and ionizing spectra in this region of the diagram. Using Eqs. (1) and (2) the values of X$_3^*$ and X$_2^*$ have been computed for all the H II regions from our compilation. The oxygen abundances (O/H)$_{Te}$ versus observed X$_{23}$ and versus computed X$_2^*$ and X$_3^*$ values are shown in Fig. 8. The (O/H)$_{Te}$ versus X$_2^*$ is shown by triangles, the (O/H)$_{Te}$ versus X$_{23}$ is presented by plusses, and (O/H)$_{Te}$ versus X$_3^*$ is shown by circles. The X$_{23}$ values are again positioned between corresponding X$_2^*$ and X$_3^*$ values. In the case of oxygen-rich H II regions the values of p_2 are usually closer to zero than those of p_3. Hence, the extrapolated intersect X_2 seems to be more reliable than the extrapolated intersect X_3 and the values of X$_2^*$ are more suitable for the oxygen abundance determination in the oxygen-rich H II regions. The dispersions in X$_2^*$ and X$_3^*$ values for a given oxygen abundance are significantly larger for oxygen-rich than for oxygen-poor H II regions.

For H II regions with 12+log$(O/H)_{Te} > 8.15$ the relations between O/H and X$_{23}$ and between O/H and X$_2^*$ have been again approximated by linear relationships. The adopted relation between O/H and X$_{23}$ (dashed line in Fig. 8) is

$$12 + log(O/H)_{R_{23}} = 9.50\text{–}1.40\ X_{23}, \quad (5)$$

and the adopted relation between O/H and X$_2^*$ (solid line in Fig. 8)

$$12 + log(O/H)_{P_2} = 9.54\text{–}1.68\ X_2^*. \quad (6)$$

The differences $\Delta log(O/H)_{P_2}$ and $\Delta log(O/H)_{R_{23}}$ as a function of p$_2$ are shown in Fig. 9. As in the case of the low-metallicity H II regions, the error in the value of oxygen abundance derived with the R_{23} – method involves two parts: a random error and a systematic error. However in the case of oxygen-rich H II regions the systematic errors are masked by large random errors. There is no systematic error in the oxygen

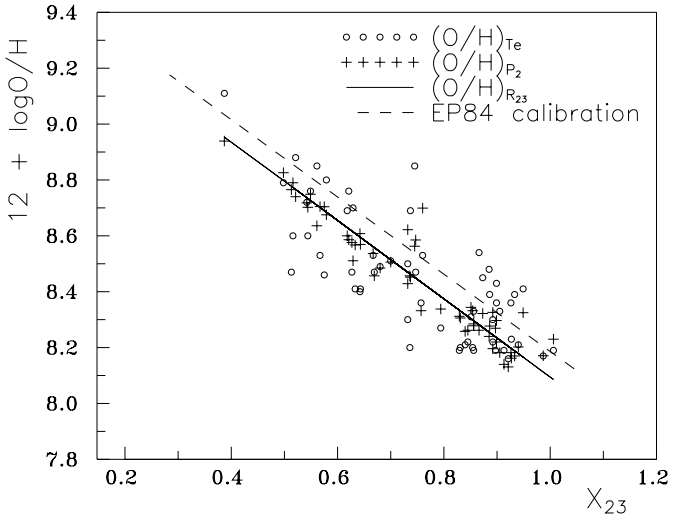

Fig. 10. The upper branch (12+logO/H > 8.15) of the X_{23} – O/H diagram. The oxygen abundances derived with the T_e – method (original data from literature) are shown by circles, the abundances derived with the suggested p – method are shown by plusses. The solid line is the O/H – R_{23} calibration obtained here, the dashed line is the O/H – R_{23} calibration from Edmunds & Pagel (1984).

abundances derived with the p – method. Thus, the determinations of oxygen abundances with the correction of R_{23} for excitation effects result in oxygen abundances which are in better agreement with oxygen abundances derived through the T_e – method both in low- and in high-metallicity H II regions.

3. Discussion

Thus, the following simple method of oxygen abundance determination based on the readily observable lines $[OII]\lambda\lambda 3727, 3729$ and $[OIII]\lambda\lambda 4959, 5007$ is suggested. Using Eq. (1) the value of $X_3^* = X_3^{obs} - \Delta X_3$ (or using Eq. (2) the value of $X_2^* = X_2^{obs} - \Delta X_2$) is derived, and then using Eq. (4) for oxygen-poor H II regions (or Eq. (6) for oxygen-rich H II regions) the value of 12 + logO/H is determined. It should be emphasized however that the linear approximations of ΔX_2 versus p_2 (ΔX_3 versus p_3) and O/H versus X_2^* (O/H versus X_3^*) relations can be a simplification of reality and more rigorous treatment can require the use of more complex curves for these relations. It is impossible to find with confidence these curves with available data and we have to use a linear approximation. Then the suggested numerical expressions should be considered as a first-order approximation.

The O/H versus X_{23} diagram for upper branch (12+log(O/H) > 8.15) is presented in Fig. 10. The oxygen abundances derived with the T_e – method (original data from literature) are shown by circles, those derived with the suggested p – method are shown by crosses, the R_{23} – O/H calibration derived here is shown by the solid line, and R_{23} – O/H calibration after Edmunds & Pagel (1984) is presented by the dashed line. In the considered range of oxygen abundances the R_{23} – O/H calibration of Edmunds & Pagel (1984) can be expressed as

$$12 + log(O/H)_{EP84} = 9.57\text{–}1.38\ X_{23}. \quad (7)$$

Inspection of Fig. 10 and comparison of Eqs. (5) and (7) shows that the R_{23} – O/H calibration derived here and that of Edmunds and Pagel have in fact the same slopes. The latter is shifted towards higher oxygen abundances by about 0.07 dex as compared to the one derived here on the basis of more recent data. Other previous calibrations (McCall et al. 1985, Dopita & Evans 1986, Zaritsky et al. 1994) are shifted towards still higher oxygen abundances.

As can be seen in Fig. 10 there is no one-to-one correspondance between X_{23} value and oxygen abundance derived with the p – method. Inspection of Fig. 9 shows that the differences between oxygen abundances derived with the p – method and with the R_{23} – method are systematically changed with p_2 from around –0.1 dex for H II regions with $p_2 \sim$ –0.1 to around +0.2 dex for H II regions with $p_2 \sim$ –1. In the general case, two H II regions (with $p_2 \sim$ –0.1 and with $p_2 \sim$ –1) can have the same $(O/H)_{R_{23}}$ while their $(O/H)_{P_2}$ can differ by ~ 0.3 dex. For H II regions with p_2 from $\sim$ –0.7 to $\sim$ –0.2 (majority of H II regions in the present compilation) these differences are appreciably less than differences between oxygen abundances derived with the R_{23} – method (or the p – method) and those derived with the T_e – method, Fig. 9. It is easy to understand that the proximity of $(O/H)_{R_{23}}$ and $(O/H)_{P_2}$ for H II regions with p_2 in the range from $\sim$ –0.7 to $\sim$ –0.2 is caused by the fact that the H II regions with p_2 values from this range lie close to the derived O/H – X_{23} relation (see discussion for low-metallicity H II regions and Fig. 7).

The exactness of oxygen abundance determination with the suggested p – method should be estimated. This can be easily done for low - metallicity H II regions where there is a large subset of homogeneous high-quality oxygen abundance determinations with the T_e – method. As it was indicated above the average value of the difference $\Delta log(O/H)_{P_3}$ is equal to 0.042 dex (by absolute value), and maximum value is around 0.1 dex. Thus, the p – method can be used for oxygen abundance determination in oxygen-poor H II regions in which the temperature-sensitive lines like $[OIII]\lambda 4363$ are measured with large uncertainty or are undetectable. For oxygen-poor H II regions the exactness of oxygen abundance determination with the p – method is comparable with the exactness provided by the T_e – method.

The estimation of an exactness of the oxygen abundance determination with the p – method in the case of the oxygen-rich H II regions (upper branch) is more problematic since few high-quality oxygen abundance determinations with the T_e – method are available. The mean value of $\Delta log(O/H)_P$ (by absolute value) for oxygen-rich H II regions is 0.14, and for an individual H II region this difference can be as large as around 0.25, Fig. 9. In the limiting case, when it is assumed that the oxygen abundances derived with the T_e – method are precise, the values of $\Delta log(O/H)_P$ are totally accounted for by the inexactness of the p – method. This seems not to be the case, as it is well known that the exactness of abundance determina-

tions in metal-rich H II regions is rather low (see present-day review in Henry & Worthey 1999). The temperature-sensitive lines like $[OIII]\lambda 4363$ used in the T_e – method are very weak in oxygen-rich H II regions and are measured with large uncertainty that results in large uncertainty in the oxygen abundances. Then the uncertainties in the oxygen abundances derived with the T_e – method can make a significant (may be a dominant) contribution to $\Delta log(O/H)_P$. In this case it can be suggested (without pretending that the p-method provides more accurate oxygen abundances than the T_e – method in principle) that the p – method (and the R_{23} – method for H II regions with low level of excitation) provides as accurate oxygen abundances in oxygen-rich H II regions as the T_e – method taking into account the present-day state-of-art with the line intensity measurements. It should be noted that if errors in $(O/H)_{Te}$ are random they impact weakly on the X_2^* – O/H and X_{23} – O/H calibrations based on the $(O/H)_{Te}$.

The biggest set of H II regions in individual galaxy with oxygen abundances determined with the T_e – method is the data of Garnett et al. (1997) for H II regions in NGC2403. Fig. 11 shows the radial distributions of oxygen abundance in NGC2403 derived by Garnett et al. (1997) with the T_e – method (circles), derived with the p – method (plusses), and derived with the R_{23} – method (Edmunds and Pagel calibration) (triangles). Inspection of Fig. 11 shows that the oxygen abundances derived with the p – method correlates even more tightly with the galactocentric distance than the oxygen abundances derived with the T_e – method. Since the level of excitation in H II regions of NGC2403 is not very high (p_3 is less than -0.2 for any H II region) the R_{23} – method (present calibration) results in the oxygen abundances which are close to that derived with the p – method. The oxygen abundances determined with calibration of Edmunds and Pagel are slightly higher than that obtained with present calibration, in agreement with above conclusion that the R_{23} – O/H calibration of Edmunds and Pagel is shifted towards higher oxygen abundances by around 0.07 dex. Thus, the case of NGC2403 confirms that the p – method and the R_{23} – method provide as accurate oxygen abundances in oxygen-rich H II regions as the T_e – method.

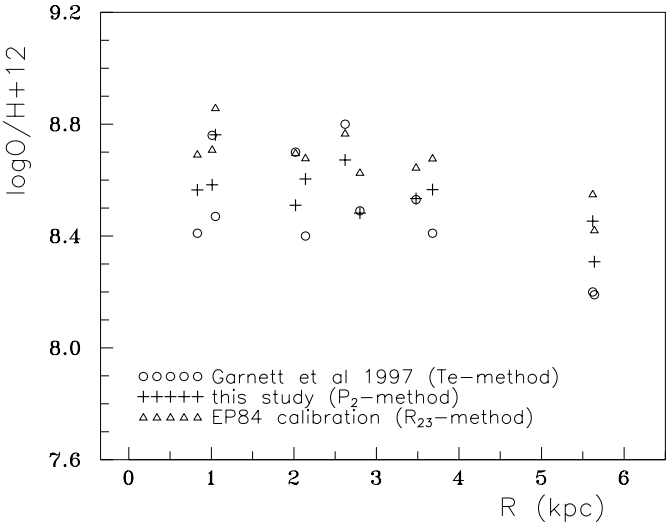

Fig. 11. The radial distributions of the oxygen abundance in NGC2403 derived by Garnett et al. (1997) with the T_e – method (circles), derived with the p – method (plusses), and derived with Edmunds and Pagel calibration (R_{23} – method).

4. Conclusions

The problem of line intensities – oxygen abundance calibration has been considered. It has been obtained that the oxygen abundances derived with the R_{23} – method involve a systematic error caused by the failure to take into account the differences in physical conditions in different H II regions.

We confirm the idea of McGaugh (1991) that the strong (readily observable) oxygen lines ($[OII]\lambda\lambda 3727,3729$ and $[OIII]\lambda\lambda 4959,5007$) contain the necessary information for determination of accurate abundances in low-metallicity (and may be also in high-metallicity) H II regions. It has been found that the excitation parameters p_3 or p_2 (which are defined here as contributions of the radiation in $[OIII]\lambda\lambda 4959,5007$ lines and in $[OII]\lambda\lambda 3727,3729$ lines to the "total" oxygen radiation respectively) allow to take into account the variations in R_{23} values among H II regions with a given oxygen abundance. Based on this fact a new way of the oxygen abundance determination in H II regions (p – method) has been constructed and corresponding relations between $[OII]\lambda\lambda 3727,3729$, $[OIII]\lambda\lambda 4959,5007$ line intensities and the oxygen abundance have been derived empirically using the available oxygen abundances determined via measurement of temperature-sensitive line ratios (T_e – method).

By comparing of oxygen abundances in H II regions derived with the T_e – method and those derived with the p – method it has been found that for the low-metallicity H II regions the exactness of oxygen abundance determination with the p – method is comparable to that obtained with the T_e – method. For the low-metallicity H II regions the p – method provides a more robust diagnostic of oxygen abundance than the R_{23} – method.

For oxygen-rich H II regions both p and R_{23} calibrations are less reliable. For the majority of H II regions in the present compilation the differences between oxygen abundances derived with the p – method and with the R_{23} – method are appreciably less than between those derived with the R_{23} – method (or the p – method) and those from the T_e – method. In the general case, however, two H II regions can have the same $(O/H)_{R_{23}}$ while their $(O/H)_{P_2}$ can differ by ~ 0.3 dex.

The calibration of R_{23} presented here is compared to previous calibrations. The calibration of Edmunds & Pagel (1984) has the same slope but is shifted towards higher oxygen abundances by about 0.07 dex as compared to the present calibration. Other previous calibrations (McCall et al. 1985, Dopita & Evans 1986, Zaritsky et al. 1994) are shifted towards still higher abundances.

For the high-metallicity H II regions the exactness of oxygen abundance determination with the suggested p – method cannot be firmly estimated due to the lack of the high-quality determinations of oxygen abundances with the T_e – method. Indirect arguments suggest that the p – method provides as ac-

curate oxygen abundances in oxygen-rich H II regions as the T_e – method taking into account the present-day state-of-art with the line intensity measurements.

Acknowledgements. I thank the referee, Prof. B.E.J.Pagel, for helpful comments and suggestions as well as improving the English text. This study was partly supported by the INTAS grant No 97–0033 and the NATO grant PST.CLG.976036.

References

Alloin D., Collin-Souffrin S., Joly M., Vigrough L., 1979, A&A 78, 200
Dopita M.A., Evans I.N., 1986, ApJ 307, 431
Edmunds M.G., Pagel B.E.J., 1984, MNRAS 211, 507
Esteban C., Peimbert M., Torres-Peimbert S., Escalante V., 1998, MNRAS 295, 401
Esteban C., Peimbert M., Torres-Peimbert S., Garcia-Rojas J., 1999a, Rev. Mex. Astron. Astrofis. 35, 65
Esteban C., Peimbert M., Torres-Peimbert S., Garcia-Rojas J., Rodriguez M., 1999b, ApJS 120, 113
Garnett D.R., Shields G.A., Skillman E.D., Sagan S.P., Dufour R.J., 1997, ApJ 489, 63
Garnett D.R., Shields G.A., Peimbert M., et al., 1999, ApJ 513, 168
Gonzalez-Delgado R.M., Perez E., Diaz A.I., et al., 1995, ApJ 439, 604
Henry R.B.C., Worthey G., 1999, PASP 111, 919
Izotov Y.I., Thuan T.X., 1998, ApJ 500, 188
Izotov Y.I., Thuan T.X., 1999, ApJ 511, 639
Izotov Y.I., Thuan T.X., Lipovetsky V.A., 1994, ApJ 435, 647
Izotov Y.I., Thuan T.X., Lipovetsky V.A., 1997, ApJS 108, 1
Kennicutt R.C. Jr., Bresolin F., French H., Martin P., 2000, astro-ph/0002180
Kobulnicky H.A., Skillman E.D., 1996, ApJ 471, 211
Kobulnicky H.A., Skillman E.D., 1997, ApJ 489, 636
Kobulnicky H.A., Skillman E.D., 1998, ApJ 497, 601
Kobulnicky H.A., Skillman E.D., Roy J.-R., Walsh J.R., Rosa M.R., 1997, ApJ 477, 679
Kwitter K.B., Aller L.H., 1981, MNRAS 195, 939
McCall M.L., Rybski P.M., Shields G.A., 1985, ApJS 57, 1
McGaugh S.S., 1991, ApJ 380, 140
Pagel B.E.J., Edmunds M.G., Blackwell D.E., Chun M.S., Smith G., 1979, MNRAS 189, 95
Pagel B.E.J., Edmunds M.G., Smith G., 1980, MNRAS 193, 219
Peimbert M., Torres-Peimbert S., Dufour R.J., 1993, ApJ 418, 760
Shaver P.A., McGee R.X., Newton L.M., Danks A.C., Pottasch S.R., 1983, MNRAS 204, 53
Shields G.A., Searle L., 1978, ApJ 222, 821
Skillman E.D., Kennicutt R.C., Shields G.A., Zaritsky D., 1996, ApJ 462, 147
Skillman E.D., Terlevich R.J., Kennicutt R.C. Jr., Garnett D.R., Terlevich E., 1994, ApJ 431, 172
Thuan T.X., Izotov Y.I., Lipovetsky V.A., 1995, ApJ 445, 108
van Zee L., Salzer J.J., Haynes M.P., O'Donoghue A.A., Balonek T.J., 1998, AJ 116, 2805
Vilchez J.M., Esteban C., 1996, MNRAS 280, 720
Vilchez J.M., Iglesias -Paramo J., 1998, ApJ 508, 248
Vilchez J.M., Pagel B.E.J., Diaz A.I., Terlevich E., Edmunds M.G., 1988, MNRAS 235, 633
Webster B.L., Smith M.G., 1983, MNRAS 204, 743
Zaritsky D., Kennicutt R.C. Jr., Huchra J.P., 1994, ApJ 420, 87